KSTLE International Journal, Vol. 1, No. 1, June 2000, pp. 1-7

Friction Characteristics of Non-Asbestos Organic (NAO) and Low-Steel Friction Materials: The Comparative Study

Seong Jin Kim and Ho Jang*

Division of Materials Science and Engineering, Korea University

Abstract : Friction characteristics of two typical friction materials (non-asbestos organic and low-steel friction materials) for an automotive brake system were investigated using an inertial brake dynamometer. In particular, the effect of sliding speed on friction coefficient was carefully investigated employing various test modes. The two friction materials were developed for commercial applications and were different mainly in the type and the amount of metallic ingredients in the friction material. The dynamometer test showed that the low-steel friction material was sensitive to the sliding speed exhibiting a negative μ-v relation. On the other hand, the non-asbestos organic friction material was less sensitive to the sliding speed. The low steel friction materials with a negative μ-v relation also induced larger vibration amplitude during brake applications.

Key words : friction material, brake, vibration, NAO, low-steel friction material, dynamometer test, stick-slip

Introduction

Performance of an automotive brake system is primarily determined by friction characteristics of a friction couple consisting of a gray cast iron rotor (or drum) and friction materials. Among many components in the brake system, the friction material, in particular, is considered as a crucial component and is often blamed for brake-induced noise and vibration. The automotive brake friction material usually contains 10-20 different raw material ingredients to meet requirements for reliable and comfortable brake performance at wide ranges of applied pressure, temperature, humidity, and sliding speed [1,2]. The individual raw material ingredient is selected for a specific friction performance during braking and synergistic effects are often achieved from 2-3 ingredients. A great deal of effort has been made to investigate the effect of each ingredient on brake-induced phenomena [3-8]. During the last several decades, systematic investigations have been carried out by friction material manufacturers, however, limited information about the roles of ingredients on friction performance are available in the literature due to proprietary reason [5,9-11].

In general, the brake friction material for a passenger car is classified as two groups [1,2]. One is a low-steel friction material (often called as a low-met friction material) and the other is a non-asbestos organic (NAO) friction material. The main difference between the two friction materials is the content of metallic constituents. The former uses 5-15 vol. % of steel fibers and the latter contains small amounts of non-ferrous metallic ingredients. It has been known that the metallic-friction material is better in terms of heat dissipation and reduces hot spotting on the rotor surface due to high thermal conductivity of steel fibers in the friction material. On the other hand, the NAO friction material shows better performance in terms of friction stability and comfort [12]. However, there are still many concerns about brake-induced problems such as noise, judder, and excessive wear of the rotor and friction materials regardless of the type of the friction material.

In this study, the two typical friction materials (low-steel and NAO) were investigated to compare the friction characteristics under various braking parameters such as applied pressure, sliding speed, and temperature. Particularly, we focused our attention to the relation between sliding speed and friction coefficient since the μ-v relation of a friction material is a very important factor in the friction performance such as brake-induced noise and vibration.

Experiments

Two different friction materials were developed for a front brake system of a mid-size passenger car and they contained typical ingredients of non-asbestos organic type and low-steel type friction materials. The major difference between the two friction materials is the type and amount of metallic constituents and other ingredients are similar. The two friction materials were developed for a commercial purpose and the NAO friction material was intended for domestic and North America markets and the low-steel friction material was designed for European exports. Raw material ingredients of the two friction materials were described in the Table 1. Only the approximate vol. % of the ingredients were given in the table due to proprietary reasons. The friction materials were manufactured by dry mixing, pre-forming, hot-pressing, post-curing, and scorching [2]. The detailed manufacturing

*Corresponding author; Tel: 82-2-3290-3276; Fax: 82-2-3290-3714
E-mail: hojang@kuccnx.korea.ac.kr

Table 1. Raw material ingredients used to produce friction material specimens A and B

Ingredients	Specimen A (vol.%)	Specimen B (vol.%)
Phenolic Resin	9 - 18	9 - 18
Aramid Fiber	5 - 8	5 - 8
Vermiculite	4 - 8	4 - 8
Cut Copper	1 - 3	0
Bronze Powder	0	1 - 3
Graphite	5 - 9	5 - 9
Steel Fiber	0	5 - 10
Rubber Powder	3 - 7	3 - 7
Cashew Particles	7 - 10	7 - 10
Barites	10 - 30	10 - 30
Ceramic Fiber	3 - 8	3- 8
Antimony Sulfide	1 - 3	1 - 3
Molybdenum Disulfide	1 - 3	1 - 3
Zirconium Silicate	3 - 5	3 - 5
Quartz Powder	1 - 2	1 - 2
Other Friction Modifier	0 - 5	0 - 5

condition can be found in the previous publications [2,13]. The final shape of the brake pad and microstructures of the two friction materials are shown in the Fig. 1. The apparent surface area of contact is approximately 58 cm^2 and the pad has a vertical slot in the center. The micrographs were acquired using a back-scattered electron image mode to obtain bright images for heavy metallic constituents. Physical properties such as surface hardness, porosity, and thermal conductivity of the two specimens were measured before friction tests and were shown in the Table 2. Table 2 shows that thermal conductivity of specimen B (low-steel) was much higher than that of specimen A (NAO) due to larger amount of steel fibers in the specimen B.

Tests for the friction performance were carried out using a singe end brake dynamometer (Model D-1900, Link Engineering) and commercial brake rotors were used as counter friction partners. A schematic diagram of the single end brake dynamometer is shown in the Fig. 2. The brake rotor was made of gray cast iron and had 31 straight vanes. The dimension of the rotor was 276 mm in diameter and 26 mm in thickness. The DTV (circumferential disk thickness variation) of the rotors were 3.8 μm (tested with specimen A) and 3.6 μm (tested with specimen B), respectively.

The test procedure for this study consists of burnish stops, stop tests at various combinations of initial brake temperatures (IBT) and applied pressures, short drag tests at different velocities, and extended drag tests (mountain drag mode). The control of the friction level was regulated under constant torque control during extended drag tests to provide the same amount of energy. Tests other than extended drag modes were carried out under constant pressure control. The detailed conditions of the dynamometer test procedure are listed in the Table 3.

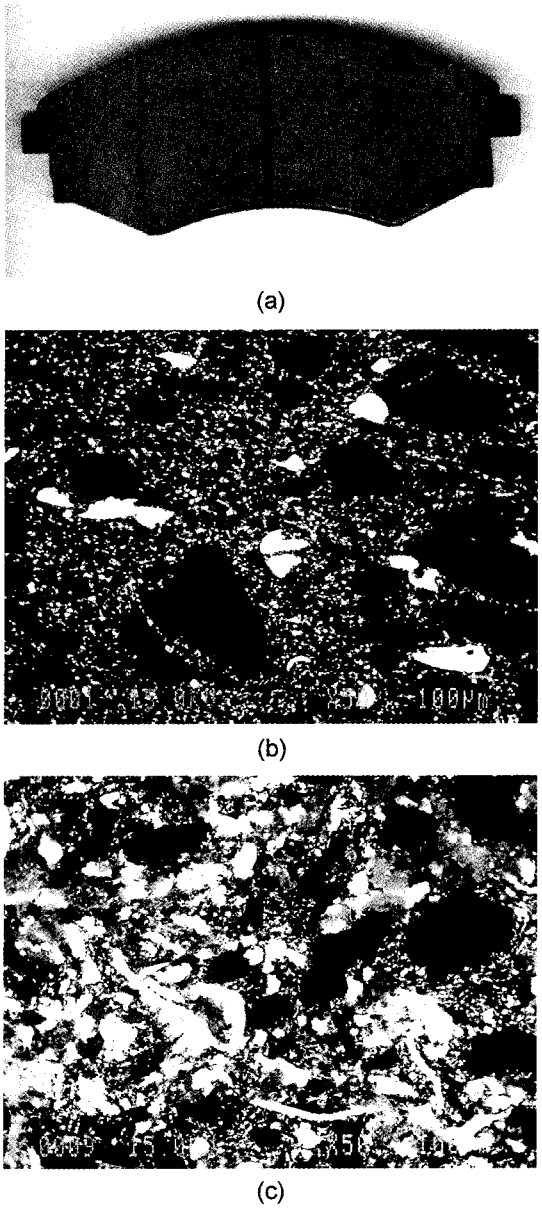

Fig. 1. The shape of the brake pad (a). The apparent surface area of contact is approximately 58 cm^2 and the pad has a vertical slot in the center. Microstructures of the two friction materials A and B are shown in (b) and (c). The micrographs were acquired using a back-scattered electron image mode to obtain bright images for heavy metallic constituents.

Results and Discussion

Friction coefficient during stop tests

Friction coefficients of the two friction materials A and B were measured during stop tests at various combinations of an applied pressure and an initial brake temperature (IBT). Fig. 3 shows the levels of friction coefficient at 25 different stop conditions. The average friction coefficients from 25 stop conditions were 0.358 and 0.352 for friction materials A and

Table 2. Physical properties of the friction materials A and B

	Specimen A	Specimen B
Hardness (Rockwell Hardness S scale)	58	54
Porosity (%) (Mercury porosimeter)	12.7	13.4
Thermal Conductivity (W/mK)	1.05	2.61

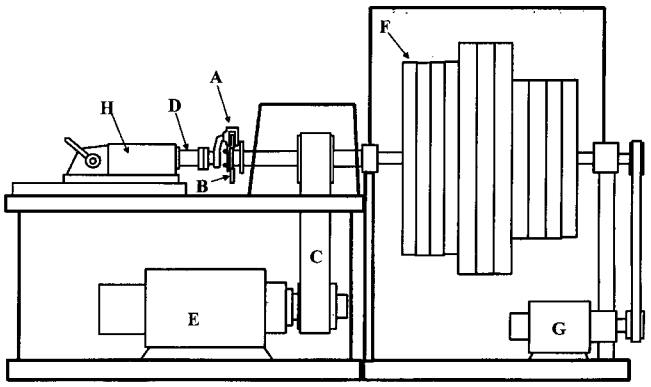

Fig. 2. A schematic diagram of the single end brake dynamometer. A: Caliper Assembly, B: Brake Rotor, C: Driving Belt, D: Torque Transducer, E: Main Driving Motor, F: Inertia Weight, G: Secondary Motor for Continuous Static Torque Measurement., H: Movable Tailstock.

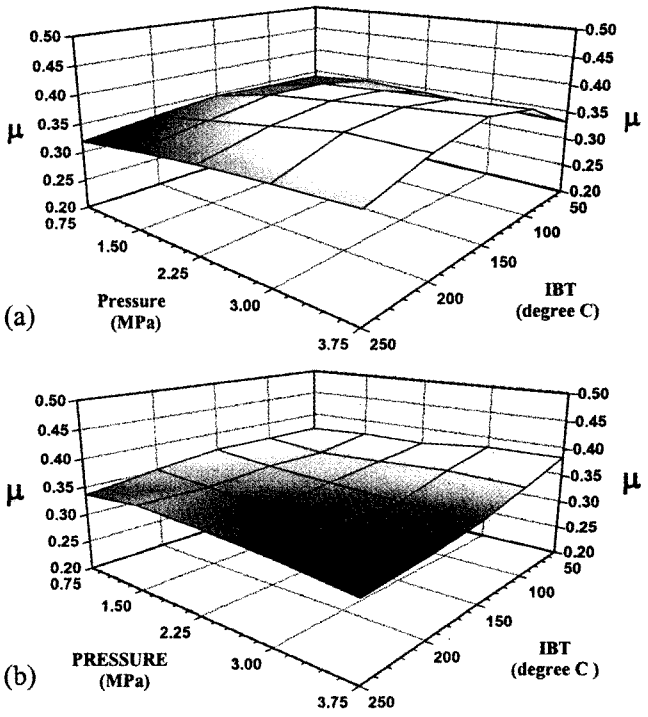

Fig. 3. Friction coefficients at 25 different stop conditions. The average friction coefficients from 25 stop conditions were 0.358 and 0.352 for friction materials A (a) and B (b), respectively. Both friction materials had excellent friction stability showing very low standard deviation (0.023 for friction material A and 0.017 for friction material B).

B, respectively. Both friction materials had excellent friction stability showing very low standard deviation (0.023 for friction material A and 0.017 for friction material B). The friction coefficient obtained from a single stop in the Fig. 3 is an average value over a time period. Therefore, it is necessary to examine the change of μ as a function of time to explore the braking characteristics in detail. A typical example of the change of friction coefficient during a stop condition (initial brake temperature = 250°C and applied pressure = 3.75 MPa) is shown in the Fig. 4. It shows that the friction coefficient with specimen B increases rapidly as the vehicle slows its speed. The steep increase of friction coefficient during a stop is called anti-fading and often causes forward jerking movement at the end of a vehicle stop and also tends to induce creep groan phenomena (low frequency vibration at very slow sliding speeds). The difference of rotor temperatures in the Fig. 4 attributes to the thermal conductivity difference of friction materials A and B. This is because the friction material B has better thermal conductivity than friction material A due to the steel fiber in the friction material B.

To investigate the anti-fading phenomena of the two friction materials, the change of the friction coefficient ($\Delta\mu$) during each stop was calculated for the 25 stop conditions. The $\Delta\mu$ value at each stop condition was obtained by subtracting the μ value at 0.3 sec (to remove unsteady initial oscillation) from the maximum μ value during a stop test at each stop condition. Fig. 5 shows the amount of anti-fading as functions of IBT and applied pressure during stop tests for two friction materials A and B, indicating that the friction material B is more susceptible to anti-fading. Less anti-fading at high initial brake temperatures in the Fig. 5(a) (friction material A) is attributed to the fact that the thermal decomposition of the friction

Table 3. Test procedure of dynamometer test employed in this study

1. Burnish stops:	IBT (100°C), Deceleration (0.35 g), Initial speed (60 km/h), Number of applications (200 times).
2. Stop tests:	IBT (50-250°C, 50°C interval), Applied pressure (0.75-3.75 MPa, 0.75 MPa interval), Initial speed (100 km/h), Total number of applications (25 stops).
3. Short drags:	IBT (50, 150, 250°C), Applied pressure (0.5, 1.0, 1.5, 2.0 MPa), Speed (10-100 km/h, 10 km/h interval), Duration (10 sec), Total number of applications (120 times).
4. Extended drags:	IBT (100°C), Torque (11 kgf·m), Speed (70 km/h), Duration (240 sec), Number of applications (10 times).

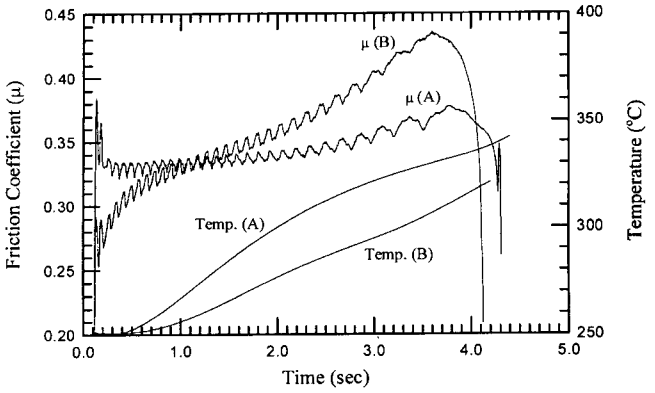

Fig. 4. An example of the change of friction coefficient during a stop condition (initial brake temperature = 250°C and applied pressure = 3.75 MPa). It shows that the friction coefficient with specimen B increases rapidly as the vehicle slows its speed.

material at high temperatures compensates the anti-fading phenomena [14-16].

Effect of sliding speed on friction coefficient

The change of friction coefficient as a function of the sliding speed is known as one of the important aspects in determining the friction characteristics during brake applications. If the friction force decreases as the sliding speed increases, an increase of vibration amplitude is often observed as a positive feedback, and vice versa [17,18]. Therefore, it is important to avoid negative μ-v slope to achieve a quiet stop. In order to investigate the effect of sliding speed on friction coefficient short drag tests (10-second duration) were carried out at different sliding speeds (10-100 km/h, 10 km/h interval) under a pressure controlled drag mode. Fig. 6 shows friction coefficient at three different sliding speeds when initial brake temperatures are 50, 150, and 250°C. The result indicates that the friction material B is more sensitive to the sliding speed and has a strong negative tendency of a μ-v relation compared to friction material A. The tendency appears stronger when the initial brake temperature is high.

Average friction coefficients during short drags were presented in Fig. 7 in terms of applied pressure and sliding speed when the IBT was 250°C. The figure clearly shows strong influence of the sliding speed on friction characteristics in the case of using the friction material B. However, the effect of applied pressure was small. When the μ-v slope of a sliding system shows a negative relation, the static friction coefficient becomes higher than dynamic coefficient of friction [19,20]. And, as a result, the friction couple causes stick-slip phenomena during sliding [19,21]. The stick-slip phenomena is known as a root cause of creep groan noise during brake applications and much effort have made to reduce the noise by modifying the formulation of the friction material or by changing the design of the brake system [17,22]. In general, the modification of a formulation is preferred to eliminate the creep groan noise since the redesign of a brake system often involves the change of a total chassis system. The ingredients

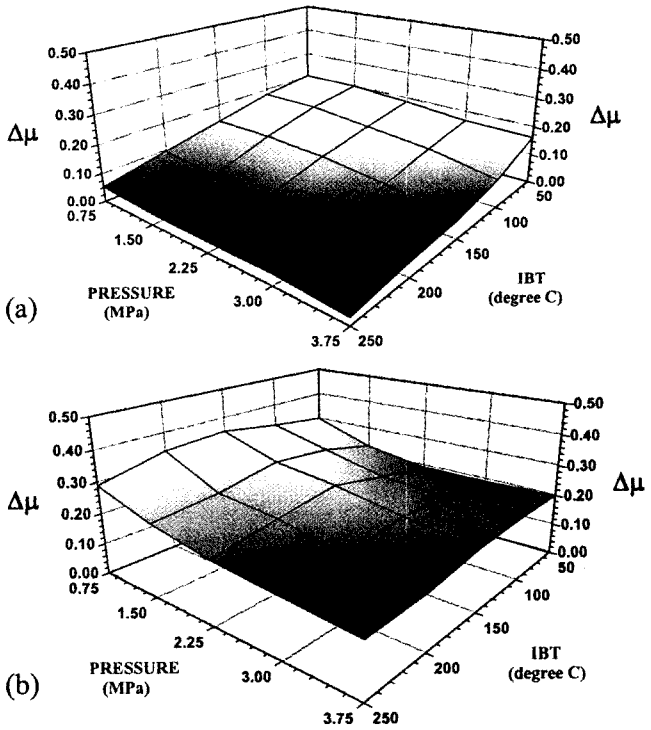

Fig. 5. Amounts of anti-fading as functions of IBT and applied pressure during stop tests for two friction materials A (a) and B (b). Average Δμ values for the friction material A and B were 0.112 and 0.236, respectively.

causing the negative μ-v slope in the friction material B was not able to identify since the friction material contained more than 10 constituents and synergistic effects among the constituents appeared to affect the anti-fading phenomena. Fig. 6 also shows that the intensity of μ variation is bigger in the case of friction material B. This is an interesting result since the rotor DTV and the rotor temperatures during drags were similar (initial rotor DTV values are 3.6 μm and 3.8 μm for rotors tested with friction materials A and B, respectively). This suggests that a friction material showing a negative μ-v slope can generate a larger amount of torque variation from stick slip phenomena during braking.

Temperature profiles during short drags were also included in the Fig. 6. The figure showed that the rotor temperatures with the friction material B were similar to or slightly higher than the rotor temperatures with the friction material A. This result is contrary to the temperature behavior during stop tests in the Fig. 4. The main reason of this difference is due to the difference in kinetic energy provided during tests. The stop test is carried out under same amount of kinetic energy using inertia wheels and the short drag test is performed under the constant pressure controlled mode. Therefore, the short drag test provides higher energy in the case of using the friction material with high average friction coefficient. The high rotor temperature with the friction material B is, therefore, due to the high input energy during drag tests and consequently compensating the better thermal conductivity of friction material B. The detailed calculation is needed to anticipate the

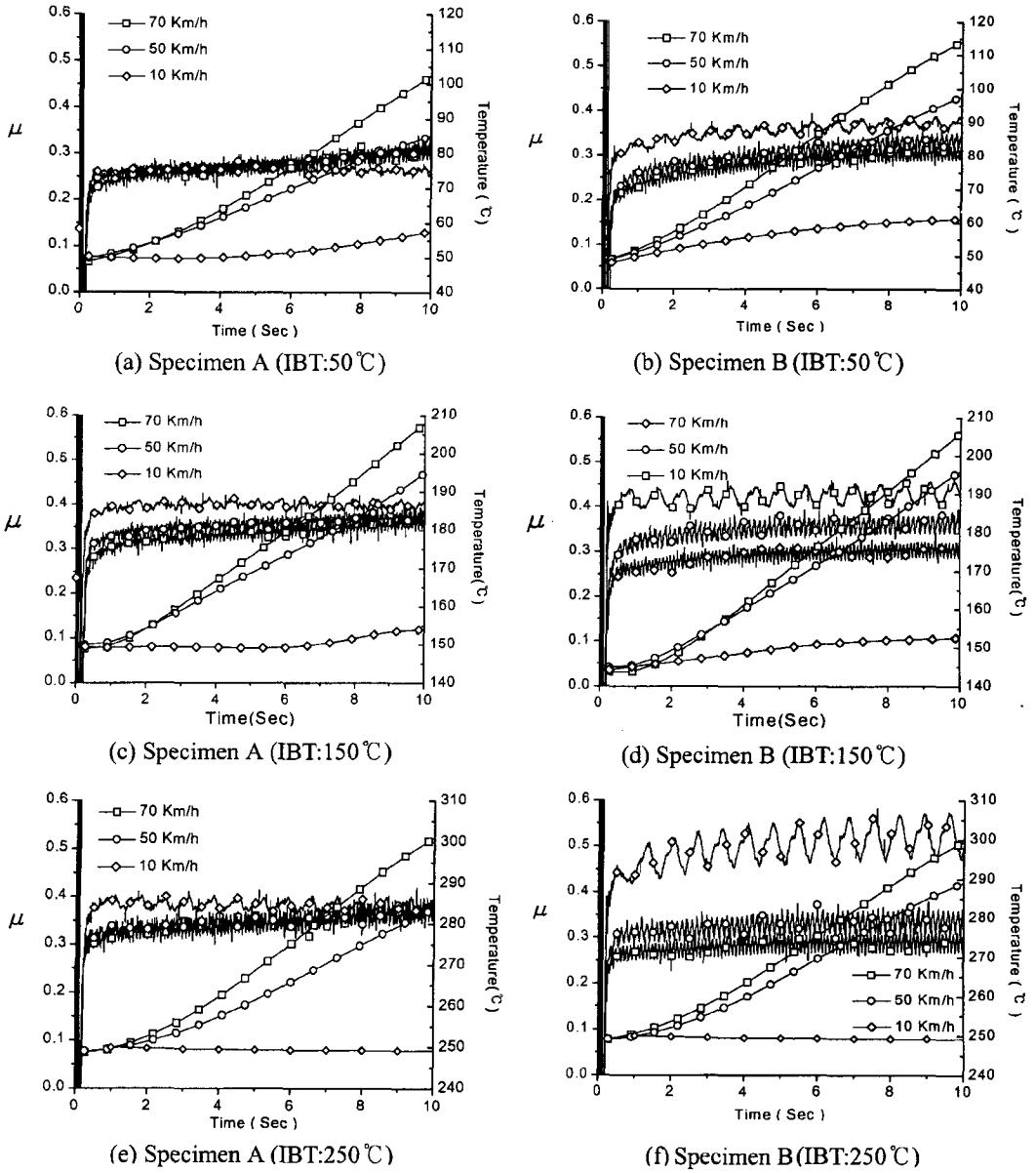

Fig. 6. Change of friction coefficient as functions of speed and initial brake temperature (IBT) for specimen A and specimen B.

temperature profile during the pressure controlled drag test considering thermal conductivity of rotor, friction material, caliper, and axel with inertial wheels. However, the temperature difference did not affect the relationship between sliding speed and the coefficient of friction.

Torque variation during extended drag tests

Extended drag tests were carried out under a constant torque control mode to examine torque variation according to the type of the friction material. The constant torque mode was chosen to provide the same amount of input energy (resulting in the same amount of friction heat) during the extended drag test. The amount of torque was set at 11 kgf·m and each extended drag test was preceded for 240 sec at 70 km/h and repeated 10 times at initial brake temperature of 100°C. Fig. 8 shows the change of friction coefficient and rotor temperature during the fifth drag cycle for friction materials A and B. The figure shows similar friction coefficients and rotor temperatures during the test. However, torque variation (torque intensity) during the fifth drag cycle shows significant difference between friction materials A and B (Fig. 9). The torque variation during a brake application is considered as one of the very important friction characteristics since the intensity of the torque variation frequently induces the brake roughness (or judder). In general, the torque variation during a brake application occurs due to the thermal distortion of disk rotors at elevated temperatures, disk thickness variation (DTV) of a rotor, and/or the uneven transfer layers on the rotor surface. In this experiment, however, it was found that the DTV values of the rotors and the rotor temperatures were similar during extended drag tests (final rotor DTV values after the tests were 4.02 μm and 3.9 μm, respectively, when the friction materials

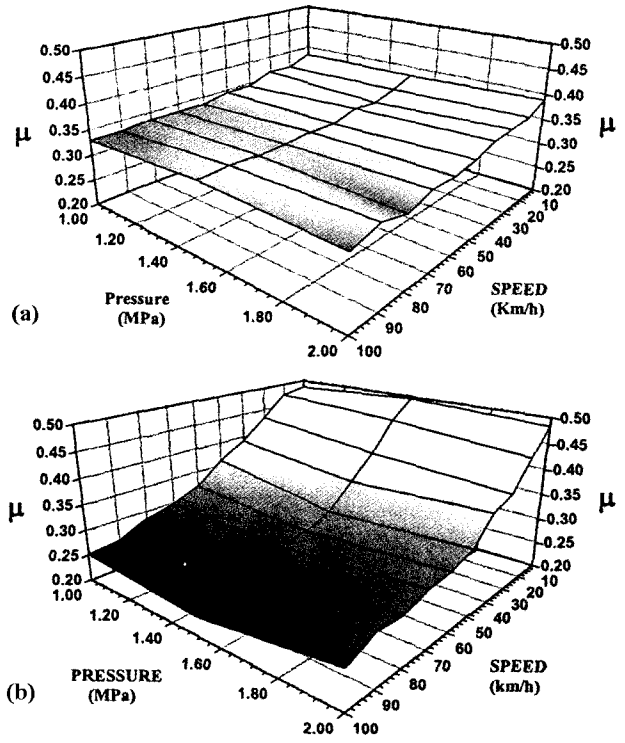

Fig. 7. Average friction coefficients during short drags were calculated as functions of applied pressure and sliding speed when the IBT was 250°C.

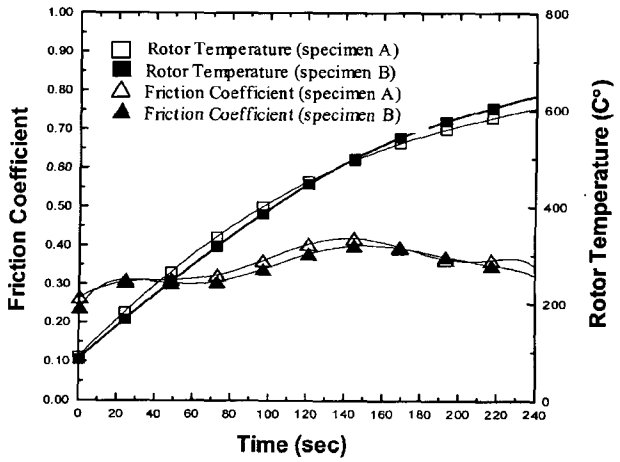

Fig. 8. Change of friction coefficient and rotor temperature during the 5th cycle of the extended drag test under torque controlled mode for friction materials A and B.

A and B were used). The observation of rotor surface also did not provide any evidence of the uneven transfer layer. In particular, the rotor surface that was tested with friction material B had shiny surfaces suggesting no transfer layer was developed on the rotor surface during the extended drag tests. This result indicates that the ingredients in the friction materials are mainly responsible for the significant difference of torque variation during extended drag tests and the friction material showing a negative μ-v slope tends to generate bigger torque variation.

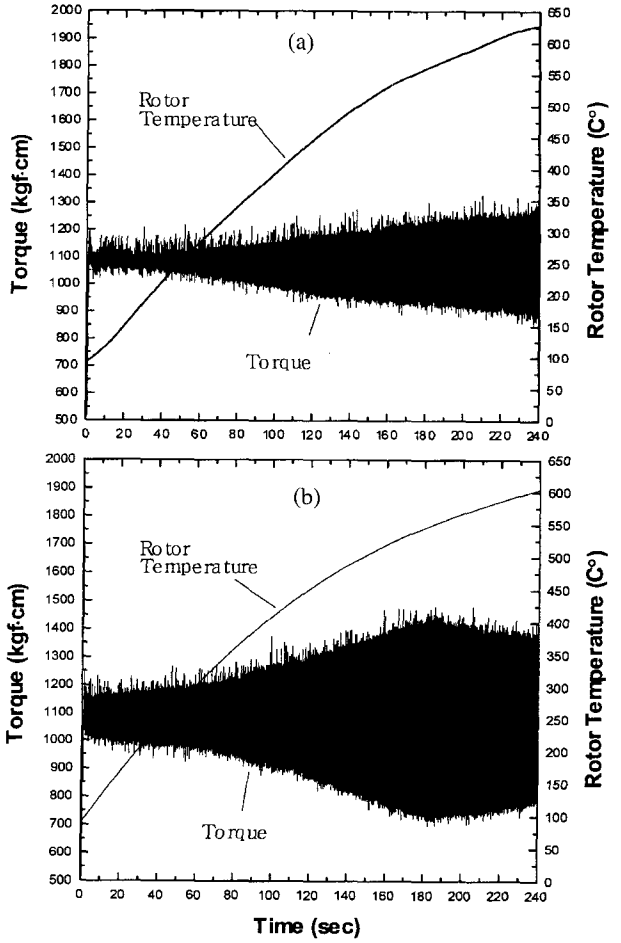

Fig. 9. Torque variation during the 5th drag cycle shows significant difference in torque intensity between friction materials A (a) and B (b).

Conclusions

Two friction materials for an automotive brake system were compared to investigate the friction characteristics. Various modes of friction tests were carried out using an inertial brake dynamometer. Test results showed that the friction material B (low-steel friction material) was strongly affected by sliding speed and exhibited typical stick-slip phenomena. On the other hand, the friction coefficient of the non-asbestos organic friction material was not strongly affected by the sliding speed. The stick-slip phenomena of the low-steel friction material induced bigger intensity of μ oscillation during the short drag tests and the effect was pronounced at slow sliding speeds. The large torque variation during stop tests and extended drag tests were also observed when the friction material B was used. This suggests that the friction material B with a strong negative μ-v relation exhibits stick-slip phenomena and tends to generate bigger torque oscillations during brake applications.

Acknowledgments

This work was supported by grant No. 98-0200-02-01-3 from the Basic Research Program of the KOSEF (Korea Science

and Engineering Foundation).

References

1. A. E. Anderson, Friction and Wear of Automotive Brakes, ASM Handbook, 19th ed., 569-577, ASM International,1992.
2. M. G. Jacko and S. K. Rhee, Brake Linings and Clutch Facings, Kirk-Othmer encyclopedia of Chemical technology, 4th ed., vol.4, pp. 523-536,1992.
3. M. G. Jacko, Physical and Chemical Change of Organic Disk Pads in Service, Wear, Vol. 46, pp.163-175, 1978.
4. Y. Handa, T. Kato, The Wear of Aramid Fiber Reinforced Brake Pads: The Role of Aramid Fibers, Tribology Transactions, Vol. 39 No. 2, 346-353, 1996.
5. L. S. Bark, D. Moran, and S. J. Percival, Chemical Changes in Asbestos-Based Friction Materials During PerformanceA Review, Wear, Vol. 34, pp.131-139, 1975.
6. M. G. Jacko, P. H. Tsang, and S. K. Lee, Wear debris compaction and friction film formation of polymer composites, Wear, Vol. 133, pp.23-38, 1989.
7. C. Blanco, J. Bermejo, H. Harsh, and R. Menendez, Chemical and physical properties of carbon as related to brake performance, Wear, 213, pp.1-12, 1997.
8. J. W. Robinson, G. E. Mogensen, K. D. Packard, J. Herman, Effect of ceramic fiber parameters on frictional performance, SAE Paper 901700, 1990.
9. N. Kamioka and H. Dokumura, U.S. Patent 5,384,344, 1995.
10. S. Das, D.C. Prevorsek, S. K. Rhee, W. J. Bulger, U.S. Patent 4,920,159, 1990.
11. T. Kudo, O. Nakajima, U.S. Patent 5,576,369, 1996.
12. A. E. Anderson, Brake System Performance-Effects of Fiber Types and Concentrations, Proceedings of Fibers in Friction Materials Symposium, The Asbestos Institute, pp.2-49, 1987.
13. H. Jang and S. J. Kim, The Effects of Antimony Trisulfide and Zirconium Silicate in the Automotive Brake Friction Material on Friction Characteristics, Wear, Vol. 239, pp.229-236, 2000.
14. H. Jang, J. J. Lee, S. J. Kim, and K. Y. Jung, The Effect of Solid Lubricants on Friction Characteristics, SAE Trans. Paper 982235, 1998.
15. L. C. Lipp, Solid Lubricants-Their Advantages and Limitations, Lubrication Engineering, Vol. 2, No. 11, pp.574-584, 1975.
16. P. W. Centers and F. D. Price, Tribological Performance of MoS_2 Compacts concerning Sulfur, Sb_2S_3 or Sb_2S_4, Wear, Vol. 129, pp.205-213, 1989.
17. J. Brecht, W. Hoffrichter, and A. Dohle, Mechanisms of Brake Creep Groan, SAE Trans., 973026, 1997.
18. K. C. Ludema, Friction, Wear, Lubrication, CRC Press, pp.69-110, 1996.
19. E. Rabinowics, Friction and Wear of Materials, 2nd ed., John Wiley & Sons, pp.105, 1995.
20. C. Gao and D. Kuhlmann-Wilsdorf, On Stick-Slip and the Velocity Dependence of Friction at Low Speeds, Transactions of ASME, Vol. 112, April, pp.354-360, 1990.
21. H. You and J. Hsia, The Influence of Friction-Speed Relation on the Occurrence of Stick-Slip Motion, Transactions of ASME, Vol. 117, July, 450-455, 1995.
22. M. Gouya and M. Nishiwaki, Study on Disk Brake Groan, SAE Paper 900007, 1990.